Original article

Size and specificity of radiopharmaceuticals for sentinel lymph node detection

Eutimio Gustavo Fernández Núñez[1], Rodrigo Teodoro[1], Danielle Pereira Wiecek[1], Natanael Gomes da Silva[2], Jose Roberto Martinelli[2] and Renato Santos de Oliveira Filho[3]

[1]Radiopharmacy Center; [2]Center of Materials Science and Technology, Institute of Energetic and Nuclear Research, Sao Paulo; [3]Faculty of Medicine, Federal University of Sao Paulo, Sao Paulo, Brazil
Correspondence to: Eutimio Gustavo Fernández Núñez. Email: eutimiocu@yahoo.com

Abstract

Background: Biological performance of radiotracers for sentinel node detection analyzed in the light of molecular design and dimension is not widely available.

Purpose: To evaluate the effect of dextran molecular size and the presence of tissue-binding units (mannose) within the model of ^{99m}Tc-carbonyl conjugate for sentinel lymph node detection.

Material and Methods: Four dextran conjugates with and without mannose in the chemical backbone were included. All polymers were radiolabeled using the precursor $[^{99m}Tc(OH_2)_3(CO)_3]^+$. Radiolabeling conditions targeted the best radiochemical purity and specific activity for each radiopharmaceutical, and partition coefficients were also defined. Lymphoscintigraphy and *ex-vivo* biodistribution in popliteal lymph node, liver and kidneys were performed in *Wistar* rats. The effects of molecular weight and mannose presence were assessed by a two-level factorial design.

Results: Radiochemical purity was indirectly related to molecular weight and presence of mannose in the polymer structure. All products were able to detect popliteal lymph node, however, uptake was strongly influenced by use of mannose (4-fold higher). Excretion was similarly modulated by differences in molecular weight. Mannose-enhanced lymph node uptake and higher molecule size in the range under study benefitted lymphoscintigraphic performance.

Conclusion: Screening of radiopharmaceuticals for lymphoscintigraphy might improve with attention to the mentioned physico-chemical features of the molecule.

Keywords: Radiopharmaceutical, sentinel lymph node, technetium, pharmacology, mannose receptors

Submitted December 2, 2010; accepted for publication March 29, 2011

Sentinel lymph node biopsy has considerably improved diagnosis of metastases of melanoma and breast cancer (1). Lymph node radiodetection is the technique of choice, and most radiopharmaceuticals use technetium-99m as the radionuclide (2). Commonly employed agents include macromolecules and colloids such as ^{99m}Tc-dextran, ^{99m}Tc-labeled human serum albumin, ^{99m}Tc-phytate, ^{99m}Tc-sulfur colloid, ^{99m}Tc-tin colloid and ^{99m}Tc-rhenium sulfide (3, 4). Nevertheless, all of these markers lack receptor specificity.

Biological performance of radiotracers may suffer interference from chemical structure, molecular size and target tissue specificity, yet few protocols have addressed these points (5).

Dextrans are suitable for lymph node radiodiagnosis, with the advantage of choice of molecular size. These polysaccharides are easily soluble, biodegradable, non-toxic and can be obtained in a variety of molecular weights (1–2000 kDa by enzymatic hydrolysis) (6).

Complex polymers containing mannose may exhibit effects on the immune system due to activation of macrophages and stimulation of T cells. Some are potent immunostimulants with significant activity against infectious diseases and tumors (7). Mannose-binding proteins are found in hepatocytes and in the spleen, lung, and lymph nodes (8), and not only on the surface of the cells but also in serum (9). Recently, a receptor-binding radiopharmaceutical for mapping sentinel lymph node has been

developed by mannose incorporation into the molecular design (10).

The novelty of this work was to quantify the effects of molecular size and presence of a tissue-binding unit (mannose) in dextran radiolabeled with ^{99m}Tc-carbonyl, evaluated by biodistribution and imaging of popliteal and inguinal lymph node in a rat model. The main difference between dextran mannose conjugates included in this study and the analogous previously reported (10) is the radiolabeling chemistry, as chelating agents are using cysteine and diethylenetriaminepentaacetic acid, respectively.

Material and Methods

Material

$Na[^{99m}TcO_4]$ was eluted from $^{99}Mo/^{99m}Tc$ generator (Institute of Energetic and Nuclear Research, IPEN/CNEN-Sao Paulo, Brazil), using 0.9% saline. $[^{99m}Tc(OH_2)_3(CO)_3]^+$ was prepared from Isolink kit (Mallinckrodt-Tyco, Petten, The Netherlands) and Vital dye for combined technique (patent blue V) was purchased from Guerbet (Rio de Janeiro, Brazil).

Four modified dextrans with chemical purity higher than 95% were graciously provided without cost by National Center for Scientific Research "Demokritos", Athens, Greece.

Two of them were 2-propylene-S-cysteine-dextrans with molecular weights of 16.6 and 30 kDa (Fig. 1a), containing 30 and 45 chelating units (cysteine), respectively. The two others were 2-propylene-S-cysteine-mannose-dextrans. Their molecular weights were 20 and 30 KDa (Fig. 1b) with 6/24 and 9/36 units of cysteine and mannose, respectively.

Twelve female Wistar EPM-1 rats were provided by the Animal Facility of IPEN-CNEN, with weight ranging from 150 g to 200 g. They were kept in cages with controlled temperature, humidity and noise, receiving industrialized chow and water ad libitum. All animal studies were performed at the Radiopharmacy Center, IPEN/CNEN-Sao Paulo, Brazil, and the protocol was approved by the Animal Welfare Ethical Committee.

Preparation of the precursor $[^{99m}Tc(OH_2)_3(CO)_3]^+$

$[^{99m}Tc(OH_2)_3(CO)_3]^+$ was prepared from Isolink kit, adding 1 mL of $Na[^{99m}TcO_4]$ (27 mCi = 1000 MBq) as per manufacturer's instructions . The pH was neutralized with 300 μL of 1M phosphate buffer/1N HCl (1:2) at the end of radiochemical reaction.

Radiolabeling of polymers

The amount of the polymer was the same in all circumstances, namely 20 μg. This mass was dissolved in 20 μl of water. Dextrans were labeled with 100 μl precursor $[^{99m}Tc(OH_2)_3(CO)_3]^+$ (2. mCi = 74 MBq) at 100°C. For molecules with mannose reaction time was 60 min and for those without only 30 min. Radiolabeling of four dextran conjugates was carried out in triplicate.

Quality control

Radiochemical purity of the ^{99m}Tc-modified dextran was determined using a combination of thin layer and paper chromatography. Thin layer chromatography (ITLC) was carried out on silica gel impregnated glass fiber sheets (ITLCTM-SG, Pall Corporation, New York, NY, USA) with Methanol/HCl (99:1) as mobile phase. Retention factors (R_f) in this chromatography system for $^{99m}TcO_4$, $[^{99m}Tc(OH_2)_3(CO)_3]^+$ and radiolabeled dextrans were 1, 1 and 0, respectively.

Paper chromatography was performed on Whatman 1 (RJM Sales Inc., New York, NY, USA) with acetone. $^{99m}TcO_4$ only migrated (Rf = 1) from the sample application point. The distance traveled by solvents in both chromatographic systems was 10 cm.

Radioactive profile of ITLC and paper strips was measured in AR-2000 radio-Thin-Chromatography Imaging Scanner (Bioscan Inc., Washington, DC, USA).

Specific activity of radiotracers was calculated by means of activity per dextran unit weight and radiochemical purity (11).

Partition coefficient of the radiotracers was evaluated in octanol/H_2O as previously described (12), after purification (>99%) by size exclusion chromatography in PD-10 column (GE Healthcare Bio-Sciences, Uppsala, Sweden). Briefly, after 1 min of vigorous agitation and separation of the phases by gravity for another 60 min, 400 μl of each phase were transferred to individual tubes and centrifuged at 5000 × g for 3 minutes for quantitative phase separation. Three equal aliquots from both phases were collected and counted in a γ counter. The partition coefficient was expressed as log P = log (activity in octanol phase/activity in water phase).

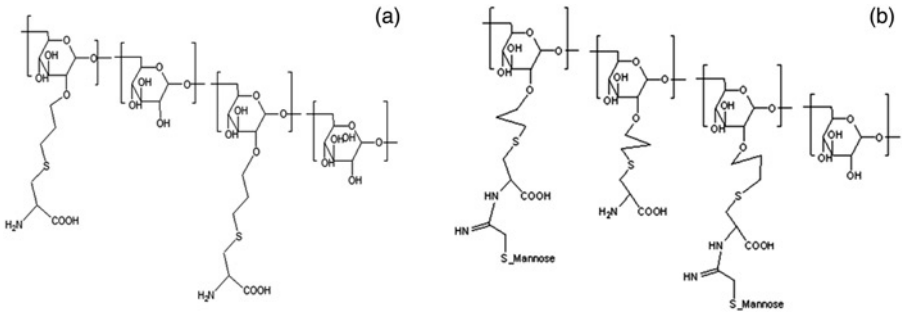

Fig. 1 (a) Basic backbone of 2-propylene-S-cysteine-dextrans. (b) Basic backbone of modified dextrans with mannose

Lymphoscintigraphy and ex-vivo uptake

Rats were anesthetized using 25 mg/kg tiletamine hydrochloride associated with 25 mg/kg zolazepam hydrochloride administered intraperitoneally. Afterwards 0.1 mL (0.17 nmol) of each radioactive preparation was subcutaneously injected in the footpad central point of the left posterior limb.

Images at 90 min post injection were performed in a Mediso Imaging System (Budapest, Hungary), employing a low-energy high-resolution collimator using a 256 × 256 × 16 matrix size with 20% energy window set at 140 keV.

A second injection with 0.05 mL vital dye was administered in the footpad in similar region of the radiotracer injection, 5 min before sacrifice time (90 min).

The popliteal region was incised permitting access and resection of the popliteal lymph node. Laparotomy with removal of kidneys and liver was done at the same time. Radioactivity of the tissues was registered by γ-counting and results were expressed as percentage of injected dose per organ (%ID).

Statistical analysis

One-way analysis of variance and Tukey's range test were performed to detect differences among radiotracer purities. A two-level factorial design was used to investigate the effects of polymer molecular weight and the presence of mannose in the chemical structure of dextran on uptake by popliteal lymph node, kidneys, and liver. Each experimental run (radiotracer assessment in rat model) was carried out in triplicate. The software used for this purpose was Statgraphics Plus 5.0 (Statistical Graphics Corp., Fairfax, VA, USA).

Results

Radiolabeling of polymers and quality control

Radiochemical purity of the radiotracers depended on polymer molecular weight and inclusion of mannose in the chemical backbone ($P = 0.0003$, ANOVA), inverse correlation being observed for both variables (Table 1). Specific activity of the molecules was distributed in a narrow range (3.34–3.61 MBq/μg) for all radiotracers (Table 1).

Table 1 Radiochemical purity and specific activity for modified dextrans

Radiotracer	Radiochemical purity (%)*	Specific activity (MBq/μg)	Log P
CD −16.6 kDa	97.57 ± 0.11†	3.61 ± 0.004	−2.208
CD −30 kDa	95.54 ± 0.90‡	3.54 ± 0.003	−2.306
CMD −20 kDa	93.26 ± 0.33§	3.45 ± 0.012	−2.040
CMD −30 kDa	90.20 ± 0.84**	3.34 ± 0.031	−2.144

*Mean ± SD
†Group 1 as Tukey's range test
‡Group 2 as Tukey's range test
§Group 3 as Tukey's range test
**Group 4 as Tukey's range test
CD = 2-propylene-S-cysteine-dextran; CMD = 2-propylene-cysteine-mannose-dextran

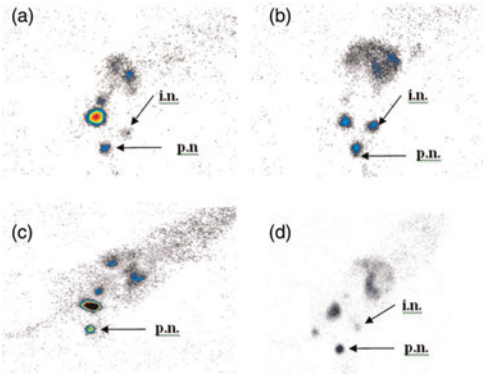

Fig. 2 Lymphoscintigraphy 90 min post injection. (a) 2-propylene-S-cysteine-dextran (16.6 kDa). (b) 2-propylene-cysteine-mannose-dextran (20 kDa). (c) 2-propylene-S-cysteine-dextran (30 kDa). (d) 2-propylene-cysteine-mannose-dextran (30 kDa). i.n. = inguinal node, p.n. = popliteal node

Also hydrophilicity of the tracers decreased with mannose presence and with decreasing molecular weight (Table 1).

Lymphoscintigraphy and ex-vivo uptake

Popliteal node identification was achieved with all products. Dissemination to inguinal lymph node occurred only with dextrans containing mannose, as well as with 2-propylene-S-cysteine-dextran of lowest molecular weight (Fig. 2).

Region of interest (ROI) of inguinal uptake of dextran-mannose was estimated by lymphoscintigraphic images. Inguinal uptake was 0.62 ± 0.06% of the injected dose for 2-propylene-cysteine-mannose-dextran (20kDa) whereas for mannose-dextran conjugate (30kDa) a lower value was documented (0.13 ± 0.09%).

Ex-vivo radiotracer uptake in popliteal lymph node, liver and kidneys can be followed in Table 2. Vital dye was used to detect the popliteal node after incision and possible modifications of tracer biodistributions caused by this dye were attenuated through its injection at a time close to the sacrifice.

Table 2 Biodistribution of radiotracers, 90 min post injection

			Tissue uptake (%)		
Run	Radiotracer	Molecular weight (kDa)	Popliteal lymph node	Kidneys	Liver
1	CMD	20	2.8	0.76	4.85
2	CMD	20	1.8	0.47	5.08
3	CMD	20	1.45	0.36	4.93
4	CMD	30	1.85	0.35	3.44
5	CMD	30	1.72	0.51	3.07
6	CMD	30	3.51	0.46	2.99
7	CD	16.6	0.65	2.42	0.57
8	CD	16.6	0.84	2.09	0.45
9	CD	16.6	0.51	2.84	0.39
10	CD	30	0.72	1.24	0.50
11	CD	30	0.41	0.91	0.70
12	CD	30	0.24	1.99	1.50

Uptakes are expressed as percentage of the injected dose (%ID)
CD = 2-propylene-S-cysteine-dextran; CMD = 2-propylene-cysteine-mannose-dextran

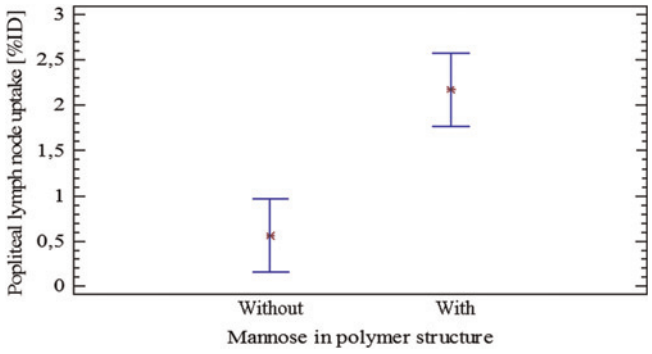

Fig. 3 Popliteal node uptake versus presence of mannose in polymer structure. Means plot. Bars define Tukey honesty significant difference intervals

The repercussions of molecular weight and mannose addition on radiotracer uptake were scrutinized by a two-level factorial design, comprising four combinations of the two variables The popliteal lymph node was statistically influenced by mannose in polymer structure ($P = 0.0018$), but not by molecular weight ($P = 0.8116$, NS) and interaction of singles factors ($P = 0.4235$, NS). In keeping with these findings, polymers with mannose showed a more robust uptake in the popliteal lymph node (four-fold higher) than without it (Fig. 3).

Kidney uptake was negatively correlated to mannose ($P = 0.0001$) and to high molecular weight ($P = 0.0215$). No conflict occurred with the factors together, which worked quite synergically ($P = 0.0427$). The opposite was true for mannose in the liver, with conspicuous elevation (5.86 fold) of uptake ($P = 1.5\ 10^{-5}$), (Fig. 4). A different pattern was shown for molecular weight ($P = 0.0044$), which exhibited reverse correlation analogously to the kidney.

Discussion

All molecules were radiolabeled according to the best conditions previously established by our group for 2-propylene-S-cysteine-dextran (16.6 kDa). In this sense, good stability at room temperature and low transchelation toward cysteine were achieved. Optimal radiolabeling conditions were 20 μg of dextran conjugate (20 μl), 74 MBq of the precursor $[^{99m}Tc(OH_2)_3(CO)_3]^+$ (100 μl), 30 min reaction time and temperature of 100°C. Only mannose-dextran conjugates demanded longer reaction time, of 60 min.

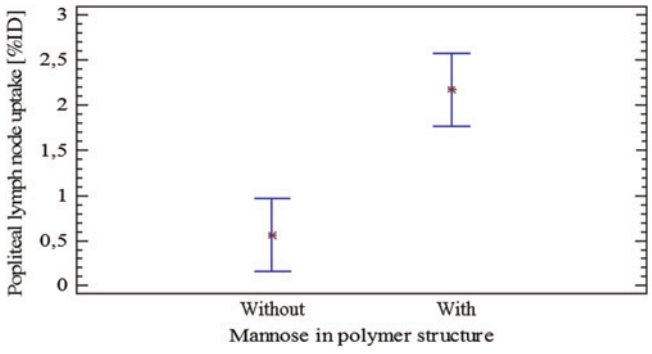

Fig. 4 Liver uptake versus presence of mannose in polymer structure. Means plot. Bars define Tukey honesty significant difference intervals

Such optimization notwithstanding, a modest decrease of radiochemical purity was observed when molecular weight increased. Less technetium-99m binding to exposed sites when the molecule has a higher molecular weight could explain such outcome. Dextrans in solution display a flexible coil conformation and the size increases linearly with molecular weight (13).

The introduction of mannose units in the dextran backbone reduces technetium chelation site number and concentration, with marked impact on radiolabeling kinetics. This explains the need to increase radiolabeling time for dextran mannose-conjugates.

Popliteal uptake was higher for dextrans with mannose (Fig. 3), because that monosaccharide upgrades lymphatic specificity of the radiotracer (14). Effect of molecular size on popliteal node uptake was ruled out for molecules with the different weights without mannose. Likewise, uptakes were not statistically different between radiotracers with mannose and dissimilar molecular weights. However, the hypothesis of lymph node saturation by the dextran mannose conjugates should not be dismissed as non-negligible uptake by the inguinal lymph node, the second one in the lymphatic chain, was observed. This phenomenon was more pronounced for smaller dextran mannose conjugate (20 kDa), demonstrating the slower migration of 2-propylene-cysteine-mannose-dextran (30 kDa).

Relative inguinal node uptake ratio between dextran-mannose 20 kDa and 30 kDa was 4.77. This finding suggests that when equal popliteal uptakes are observed, inguinal node participation has to be accounted for. Of course lymphoscintigraphy is benefited when a large fraction of the tracer is retained in the first node (15).

Our experimental strategy could contribute to the development of new radiopharmaceuticals, taking advantage of the knowledge about new lymphangiogenic markers in sentinel lymph nodes and the impact of dextran conjugates size.

The influence of specificity units (mannose) and molecular size on radiotracer uptakes in kidneys and liver was also studied. The purpose was to infer the likely effects of both variables on pharmacokinetic pattern.

The liver has receptors for mannose-terminated glycoproteins in both nonparenchymal and parenchymal cells (16), like the surface of macrophage cells. For this reason uptake of dextran-mannose conjugates is higher than 2-propyl-S-cysteine-dextrans (Fig. 4). Such indirect biological specificity overlaps with less hydrophilicity of dextran-mannose conjugates when compared to other modified dextrans (Table 1). Still, partition coefficients are not sufficiently different to explain the high liver uptakes of dextran-mannose conjugates.

The impact of the molecular weight was mainly observed in the form of radiotracer blood concentration increasing by transferring from lymphatic fluid. This statement is indirectly confirmed by the higher uptakes of 2-propyl-S-cysteine-dextrans and 2-propylene-S-cysteine-mannose-dextrans with

lower molecular weight in kidneys and liver. As a consequence they will have a faster excretion compared with analogous polymer with higher molecular weight. Such phenomenon is well documented in pharmacological studies with the dextran polymer (17). In addition, mannose units in dextran conjugates change the renal excretion of radioconjugates without this monosaccharide to hepatic excretion (Table 2).

In conclusion, the influence of size and specificity of dextran conjugates for lymph node sentinel detection was effectively assessed in rats by a two-level factorial design. Mannose in the backbone of the molecule enhanced popliteal lymph node uptake, and higher molecule size improved lymphoscintigraphic performance. The same methodological tools, rat model and factorial design, are recommended for assays of new radiopharmaceuticals for sentinel lymph node detection.

ACKNOWLEDGEMENT

The authors are indebted to the National Commission for Nuclear Energy (CNEN, São Paulo, Brazil), National Counsel of Technological and Scientific Development (CNPq, Brasília, Brazil) and the International Atomic Energy Agency (IAEA, Vienna, Austria) for scientific grants. We thank Dr I Pirmettis and his collaborators at NCSR Demokritos, Greece, for providing the modified dextrans and Drs Bluma L Faintuch and Adriano Duatti for their technical support. The corresponding author is grateful to Relma Tavares de Oliveira Fernández and to PhD Rodolfo Valdés Véliz, for inspiration to write this paper.

Conflict of interest: None.

REFERENCES

1 Taback B, Hashimoto K, Kuo CT, *et al.* Molecular lymphatic mapping of the sentinel lymph node. *Am J Pathol* 2002;**161**:1153–61
2 Seo Y, Mari C, Hasegawa BH. Technological development and advances in single-photon emission computed tomography/computed tomography. *Semin Nucl Med* 2008;**38**:177–98
3 Jain R, Dandekar P, Patravale V. Diagnostic nanocarriers for sentinel lymph node imaging. *J Controlled Release* 2009;**138**:90–102
4 Fernández Núñez EG, Faintuch BL, Teodoro R, *et al.* Influence of colloid particle profile on sentinel lymph node uptake. *Nucl Med Biol* 2009;**36**:741–7
5 Liu S. Bifunctional coupling agents for radiolabeling of biomolecules and target-specific delivery of metallic radionuclides. *Adv Drug Delivery Rev* 2008;**60**:1347–70
6 Castellanos Gil E, Iraizoz Colarte A, El Ghzaoui A, *et al.* A sugar cane native dextran as an innovative functional excipient for the development of pharmaceutical tablets. *Eur J Pharm Biopharm* 2008;**68**:319–29
7 Tizard IR, Carpenter RH, McAnalley BH, *et al.*. The biological activities of mannans and related complex carbohydrates. *Mol Biother* 1989;**1**:290–6
8 Morio H, Kurata H, Katsuyama R, *et al.* Renal expression of serum-type mannan-binding protein in rat. *Eur J Biochem* 1997;**243**:770–4
9 Wagner S, Lynch NJ, Walter W, *et al.* Differential expression of the murine mannose-binding lectins A and C in lymphoid and nonlymphoid organs and tissues. *J Immunol* 2003;**170**:1462–5
10 Wallace AM, Hoh CK, Limmer KK, *et al.* Sentinel lymph node accumulation of Lymphoseek and Tc-99m-sulfur colloid using a "2-day" protocol. *Nucl Med Biol* 2009;**36**:687–92
11 Zeevaart JR, Olsen S. Recent trends in the concept of specific activity: Impacton radiochemical and radiopharmaceutical producers. *Appl Radia Isotopes* 2006;**64**:812–4
12 Okarvi SM, Al Jammaz I. Synthesis and evaluation of a technetium-99m labeled cytotoxic bombesin peptide conjugate for targeting bombesin receptor-expressing tumors. *Nucl Med Biol* 2010;**37**:277–88
13 Rabanel JM, Hildgen P. Preparation of hydrogel hollow particles for cell encapsulation by a method of polyester core degradation. *J Microencapsulation* 2004;**21**:413–31
14 Vera DR, Wisner ER, Stadalnik RC. Sentinel node imaging via a nonparticulate receptor-binding radiotracer. *J Nucl Med* 1997;**38**:530–5
15 Vera DR, Wallace AM, Hoh CK, *et al.* A synthetic macromolecule for sentinel node detection: ^{99m}Tc-DTPA-Mannosyl-Dextran. *J Nucl Med* 2001;**42**:951–9
16 Praaning-Van Dalen DP, DeLeeuw AM, Brouwer A, *et al.* Rat liver endothelial cells have a greater capacity than Kupffer cells to endocytose yV-acetylglucosamineand mannose-terminated glycoproteins. *Hepatology* 1987;**7**:672–9
17 Behe M, Du J, Becker W, *et al.* Biodistribution, blood half-life, and receptor binding of a somatostatin–dextran conjugate. *Med Oncol* 2001;**18**:59–64